

Uncertainties in Prediction of Streamflows Using SWAT Model – Role of Remote Sensing and Precipitation Sources

Penman-Monteith's method (eqn. S1) calculates Evapotranspiration based on temperature, radiation from the Sun, Precipitation, wind velocity, and humidity, while the other two methods require only air temperature and radiation in conjunction with Precipitation to predict the Evapotranspiration.

Equation S1: Penman-Monteith Equation

$$E_o = \frac{\delta(h_o + S) + \left[\frac{\rho_a C_p (e_s - e_a)}{r_a}\right]}{HV[\delta + \gamma\left(\frac{r_a - r_c}{r_a}\right)]} \quad \dots (S1)$$

Where E_o , Evaporation in $\text{gm}^{-2}\text{s}^{-1}$; δ , slope density of saturated vapor in $\text{gm}^{-3}\text{C}^{-1}$; h_o , net radiation in $\text{Jm}^{-2}\text{s}^{-1}$; HV , Latent heat of vaporization in Jg^{-1} ; S , soil heat flux in $\text{Jm}^{-2}\text{s}^{-1}$; γ , psychometric constant in $\text{gm}^{-3}\text{C}^{-1}$; ρ_a , the density of air in gm^{-3} ; C_p , specific heat of the air in $\text{Jg}^{-1}\text{C}^{-1}$; e_s , the density of saturated vapor in gm^{-3} ; e_a , the density of vapor in gm^{-3} ; r_a , the aerodynamic resistance in sm^{-1} ; and r_c , canopy resistance in sm^{-1} .

The Priestley-Taylor and Hargreaves Evapotranspiration equations are provided in the Supplementary material.

Equation S2: Priestley-Taylor Equation

$$E_o = 1.28 \left(\frac{h_o}{HV}\right) \left(\frac{\delta}{\delta + \gamma}\right) \quad \dots (S2)$$

Equation S3: Hargreaves Equation

$$E_o = 0.0032 \left(\frac{SR_{max}}{HV}\right) (T + 17.8)(T_{max} - T_{min})^{0.6} \quad \dots (S3)$$

Where, SR_{max} is the maximum solar radiation, T_{max} and T_{min} are respective maximum and minimum temperatures in $^{\circ}\text{C}$.

The SWAT model's predictive ability was checked by applying the model to different topographic and climatic regions.

The 334 km² Little River Watershed (LRW) near Tifton, Georgia, is typical of the heavily vegetated, slow-moving stream systems found in the United States Coastal Plain Region. Land use is approximately 40% woodland within the watershed, 36% row crops (primarily peanuts and cotton), 18% pasture, and 4% water. The watershed is built on sands, silts, and clay underlain by the limestone that makes up the Floridian aquifers. The watershed's major soil series are loamy sands with about 5 cm/hr infiltration rates. Upland slopes range from 2 to 5% within the watershed, while channel slopes range from 0.1 to 0.5 percent. Precipitation falls almost entirely as rain, with an annual mean of 1200 mm in Tifton, Georgia. The rainfall distribution throughout the year is highly variable, except for the typically dry fall months. Water balance studies on the watershed show that streamflow accounts for about 30% of annual rainfall, evapotranspiration accounts for 70%, and percolation to deep groundwater is negligible. The streamflow comprises direct surface runoff (which accounts for 6 percent of annual rainfall) and returns flow from the shallow aquifer (24 percent of annual rainfall).

The Baron Fork watershed is located in the southwestern part of the Springfield Plateau Physiographic Province. The topography is gently rolling hills, with local relief around 200 feet from the ridgeline to the adjacent valley floor. Runoff is visually appealing. The Baron Fork watershed receives 44 inches of precipitation each year, most of which falls as rain. The Baron Fork is geologically underlain by fine- to coarse-grained limestones and cherty limestones of the Mississippian age Boone Formation. Historically, the stream was mined for gravel.

The South Fork of the Iowa River is the watershed of interest in Hardin and Hamilton Counties, Iowa. The watershed's total drainage area is approximately 78,000 ha, and the watershed area to be evaluated is approximately 76,250 ha. Tipton Creek (19,850 ha), Beaver Creek (18,200 ha), and the upper South Fork are the major sub-basins (25,600 ha).

The landscape is made up of glacial till deposited 10-15,000 years ago. In the watershed's upper reaches, the terrain is poorly dissected, and internally drained "prairie potholes" are common. The low relief causes poor drainage, and hydric soils cover 54% of the watershed area. The upper part of the watershed is traversed by a significant lateral moraine of the Des Moines Lobe. Subsurface tile drains, and ditches were first installed more than a century ago. Several dissolved contaminants are transported more quickly as a result of artificial drainage. The average annual precipitation is 750 mm, with 60 percent falling in short but intense events from May to August. Annual baseflow accounts for 60% of total stream discharge. The majority of the remaining runoff comes from subsurface drain inlets. Approximately 85 percent of the watershed is under corn and soybean rotation, with the remaining 6 percent under grass (CRP) and pasture. The majority of the remainder is roadways and developed land cover, with only about 1% being forest or wetland. There are approximately 100 confined swine-feeding operations in Tipton Creek and the upper South Fork, with the majority of them located in Tipton Creek and the upper South Fork.

References

- National Resources Conservation Service – United States Department of Agriculture
- Tomer, M.D., and D.E. James. 2004. Do soil surveys and terrain analyses identify similar priority sites for conservation? *Soil Sci. Soc. Am. J.* 68:1905-1915.

- Tomer, M.D., D.E. James, and T.M. Isenhardt. 2003. Optimizing the placement of riparian practices in a watershed using terrain analysis. *J. Soil & Water Conserv.* 58(4):198-206.

RESULTS – SOURCE UNCERTAINTY

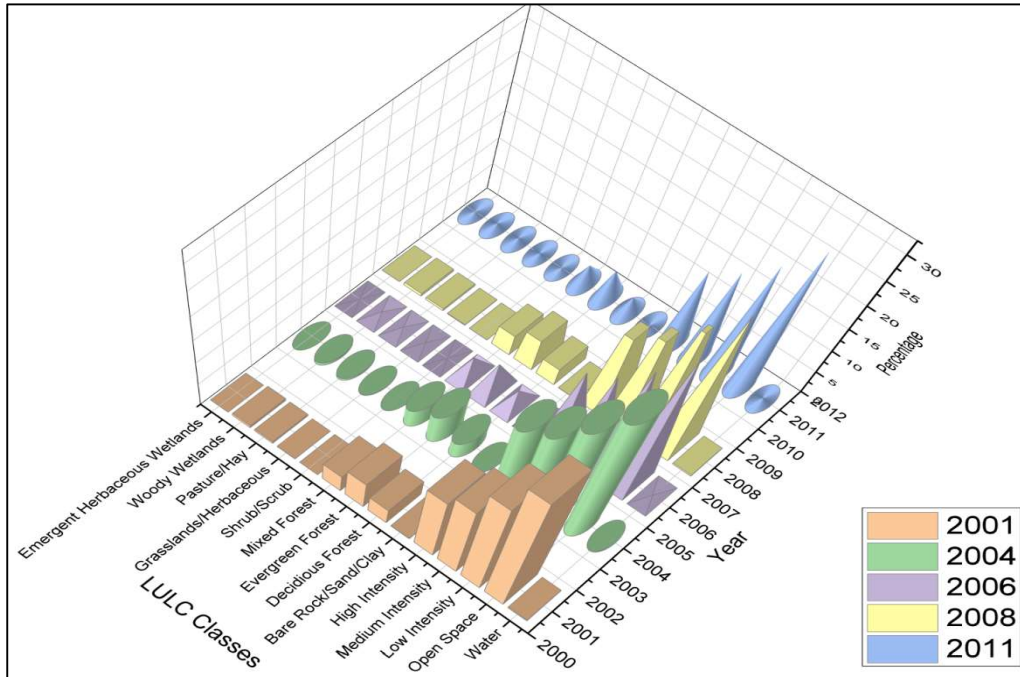


Figure S1: Comparison of NLCD LULC classes obtained for Peachtree Watershed from different years

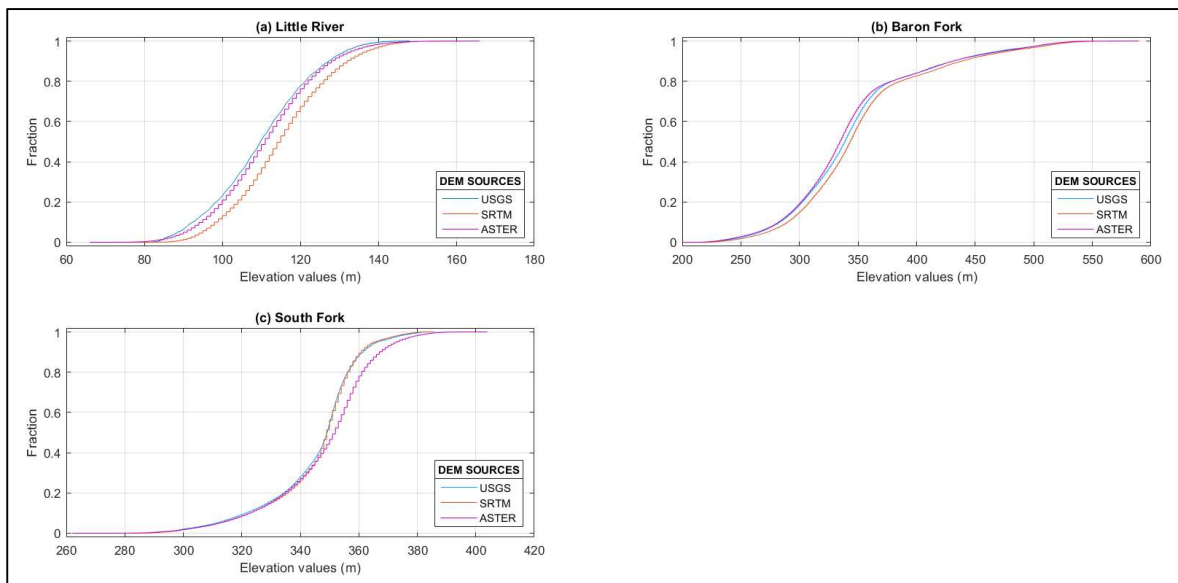


Figure S2: Minimum and Maximum elevation ranges plotted for different DEM sources showcasing uncertainty in the data for different topographical/climatic regions: (a) Little River (b) Baron Fork (c) South Fork

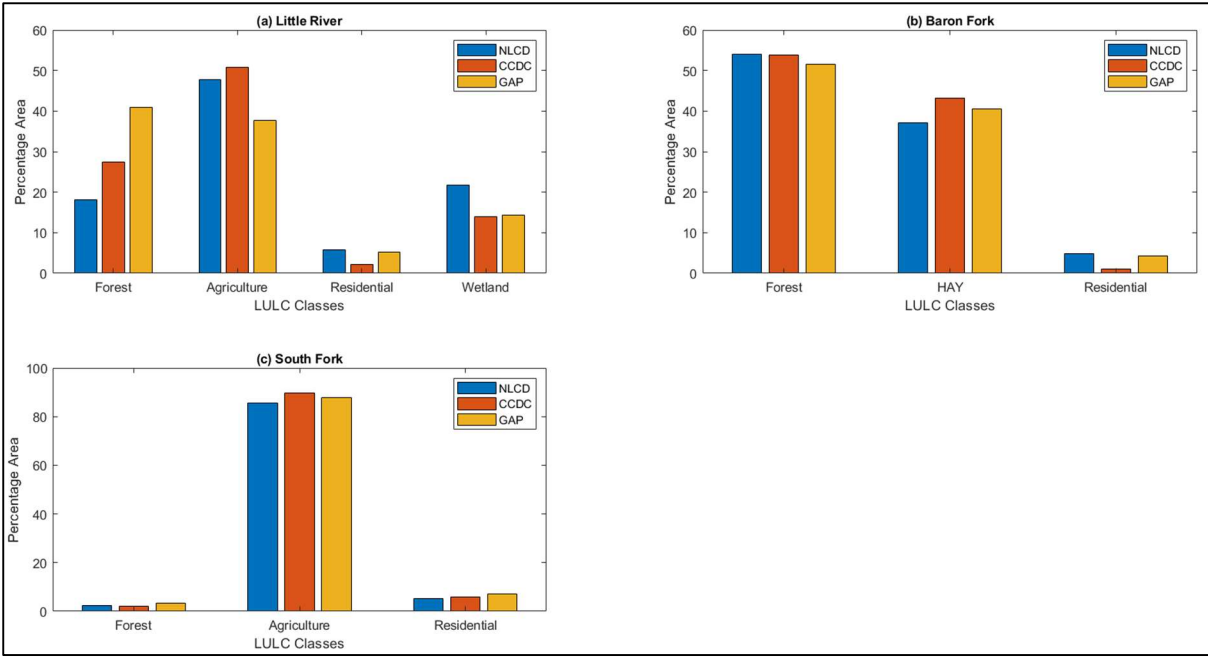


Figure S3: Comparison of major land use classes from different LULC sources like NLCD, CCDC, and GAP to get an overview of the variation in the input LULCs

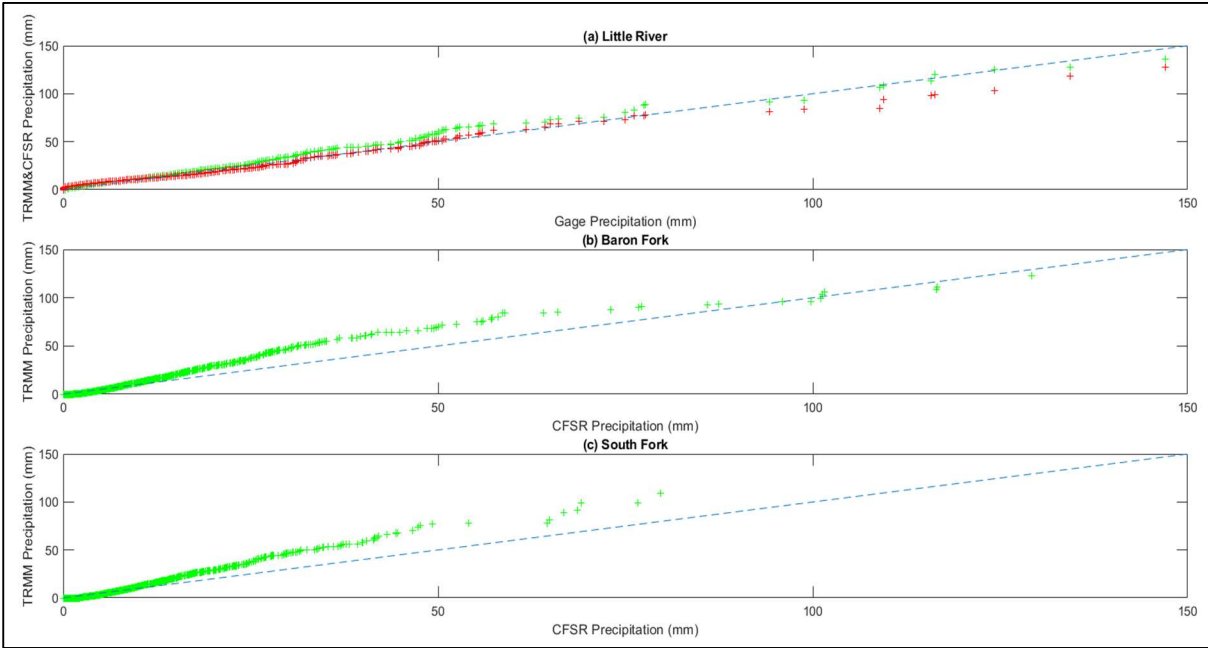


Figure S4: q-q plots for daily precipitation data comparing TRMM and CFSR data with Gage for the a) Little River watershed, while q-q plots are comparing CFSR and TRMM for the other two watersheds (b & c)

LITTLE RIVER EXPERIMENTAL WATERSHED RESULTS

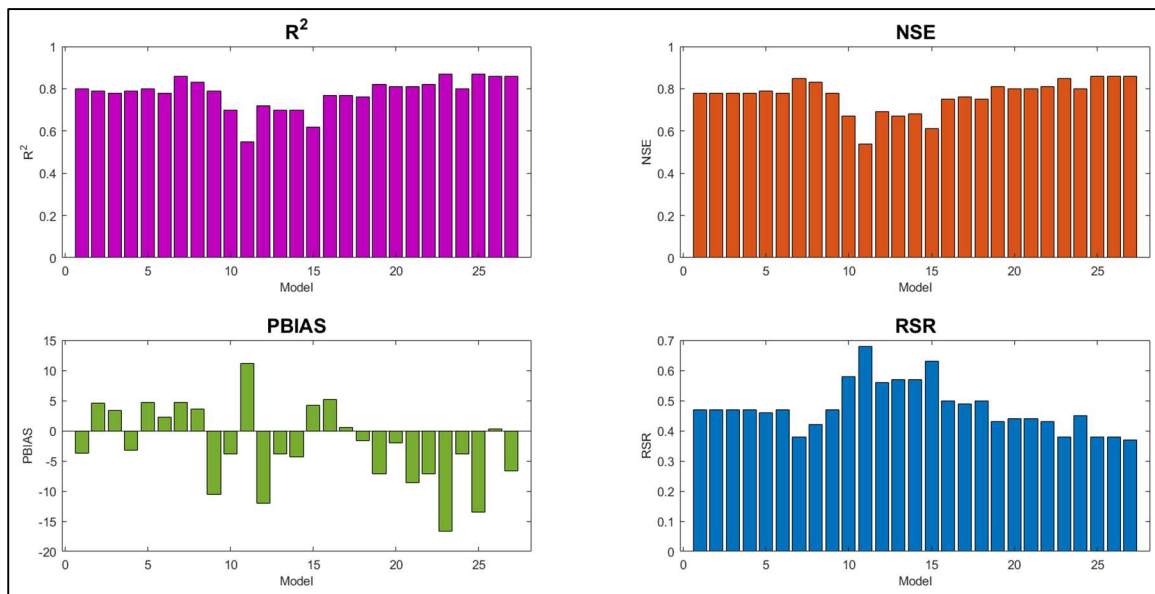


Figure S5: SWAT model performance for the 27 combinations with the four performance criteria (R^2 , NSE, PBIAS, and RSR) for the calibration period

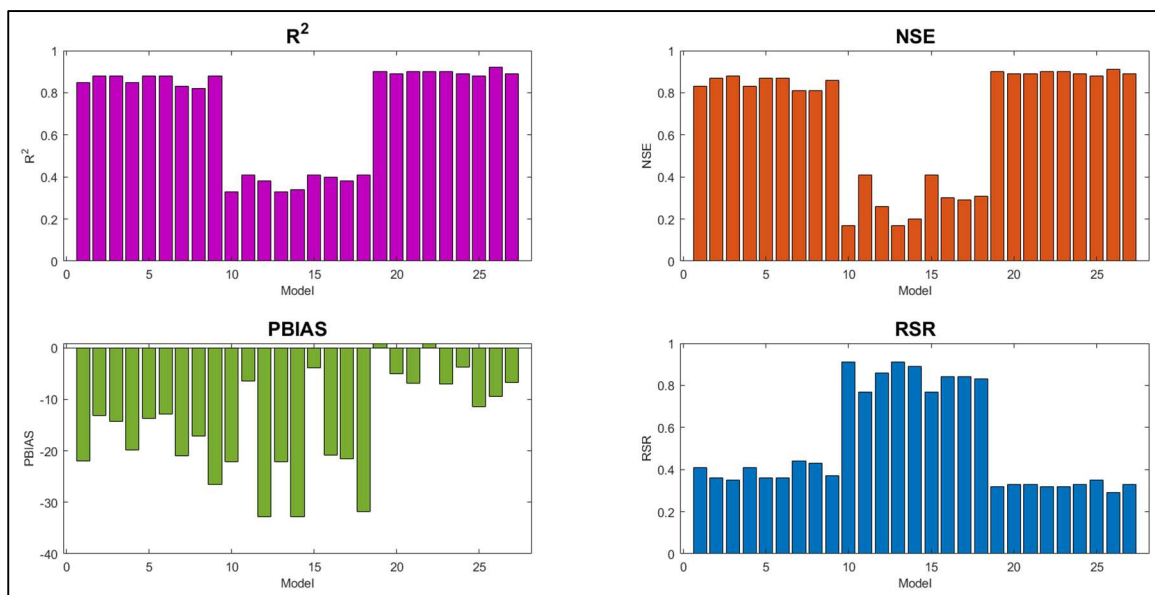


Figure S6: SWAT model performance for the 27 combinations with the four performance criteria (R^2 , NSE, PBIAS, and RSR) for the validation period

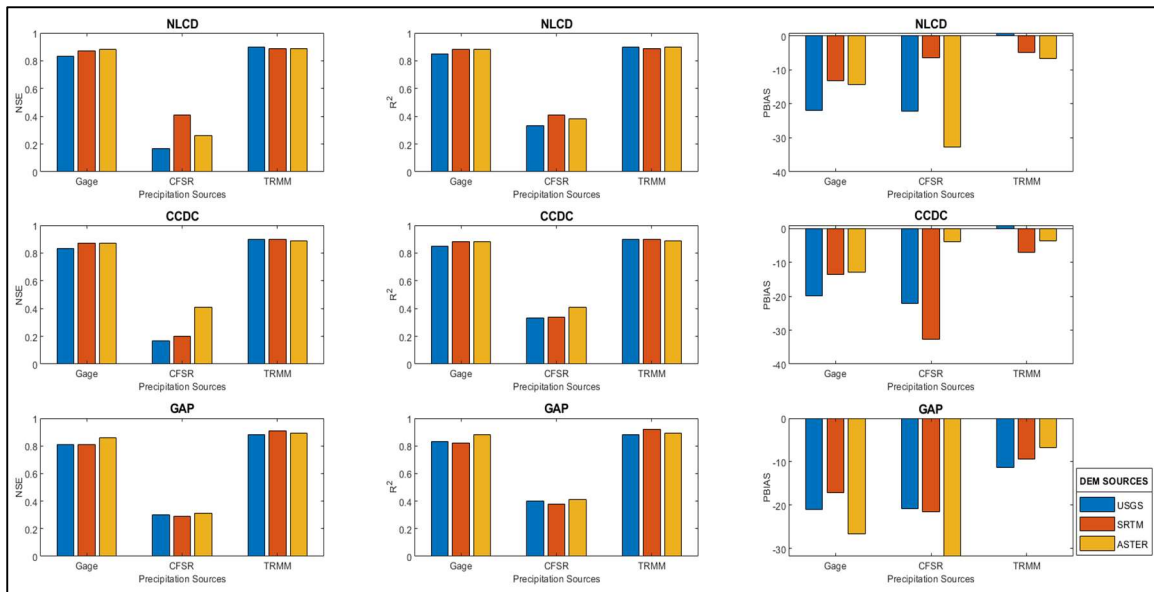


Figure S7: DEM and precipitation dataset comparison based on NSE, R^2 , and PBIAS values for (a) NLCD; (b) CCDC; and (c) GAP LULC

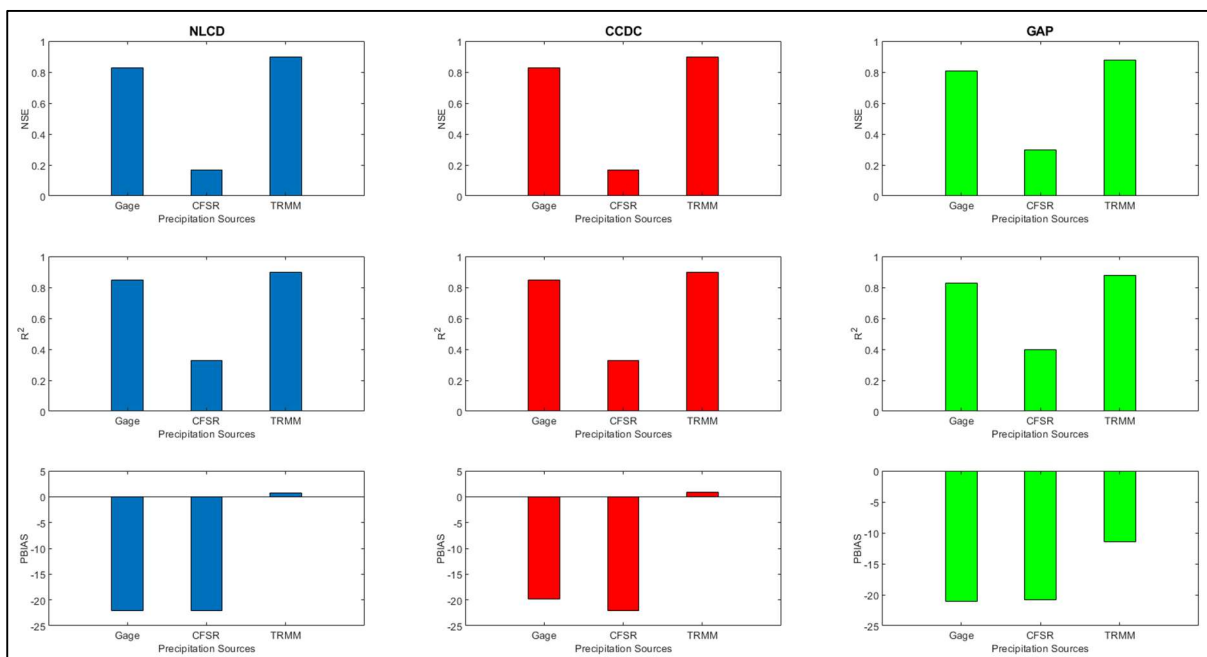


Figure S8: Model performance with various LULC and precipitation dataset combinations for the USGS DEM based on NSE, R^2 , and PBIAS criteria

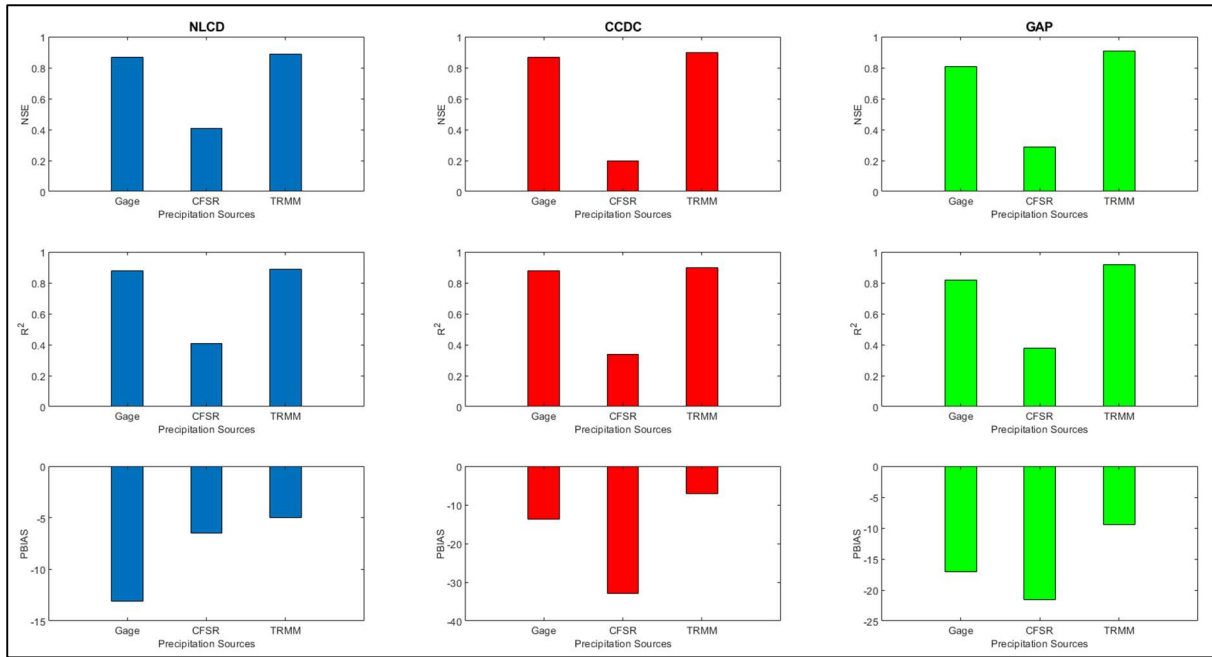


Figure S9: Model performance with various LULC and precipitation dataset combinations for the SRTM DEM based on NSE, R², and PBIAS criteria

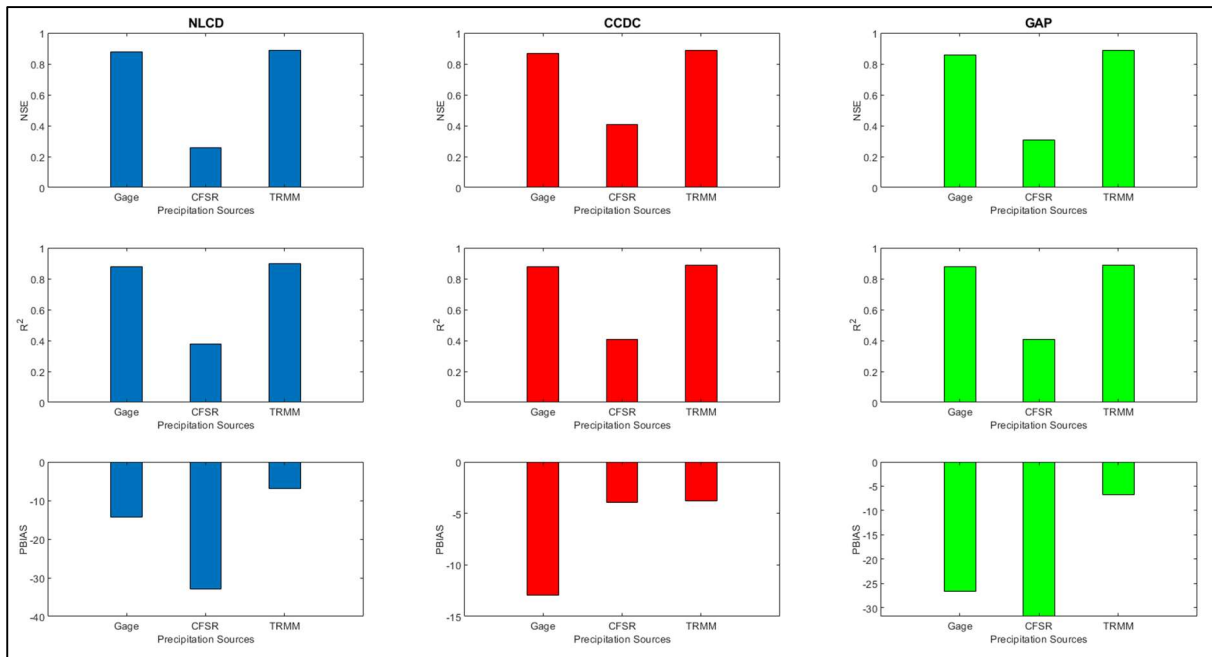


Figure S10: Model performance with various LULC and precipitation dataset combinations for the ASTER DEM based on NSE, R², and PBIAS criteria

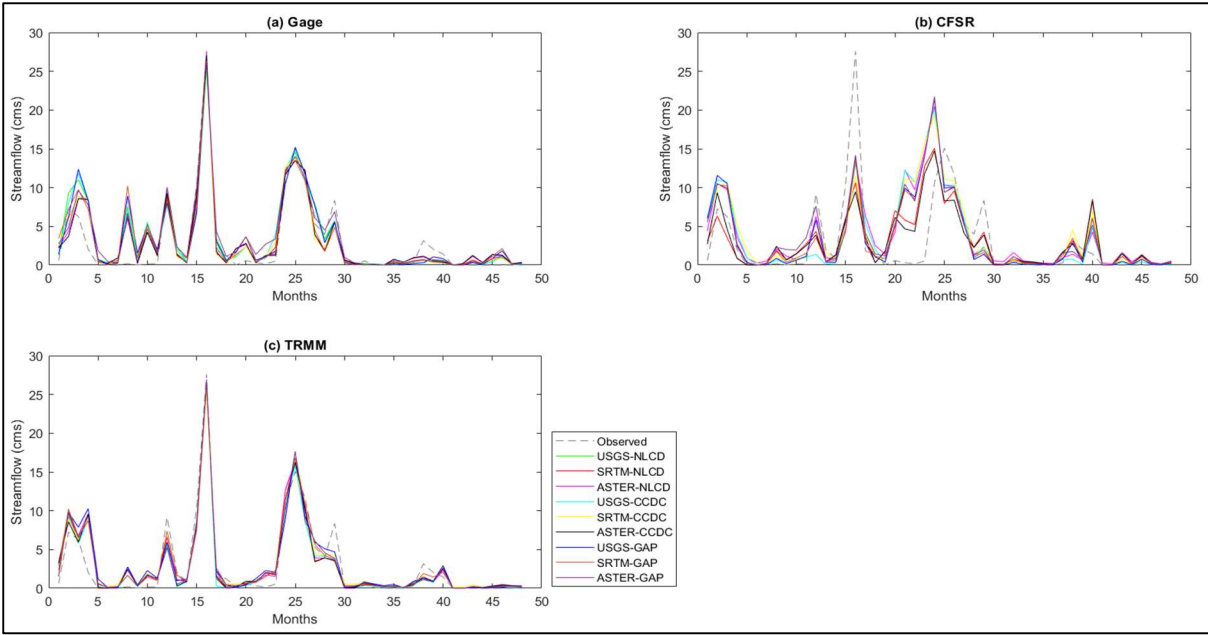


Figure S11: Plots showing the variation of simulated streamflow with the observed streamflow for three different precipitation combinations as (a) Gage (b) CFSR (c) TRMM

BARON FORK WATERSHED RESULTS

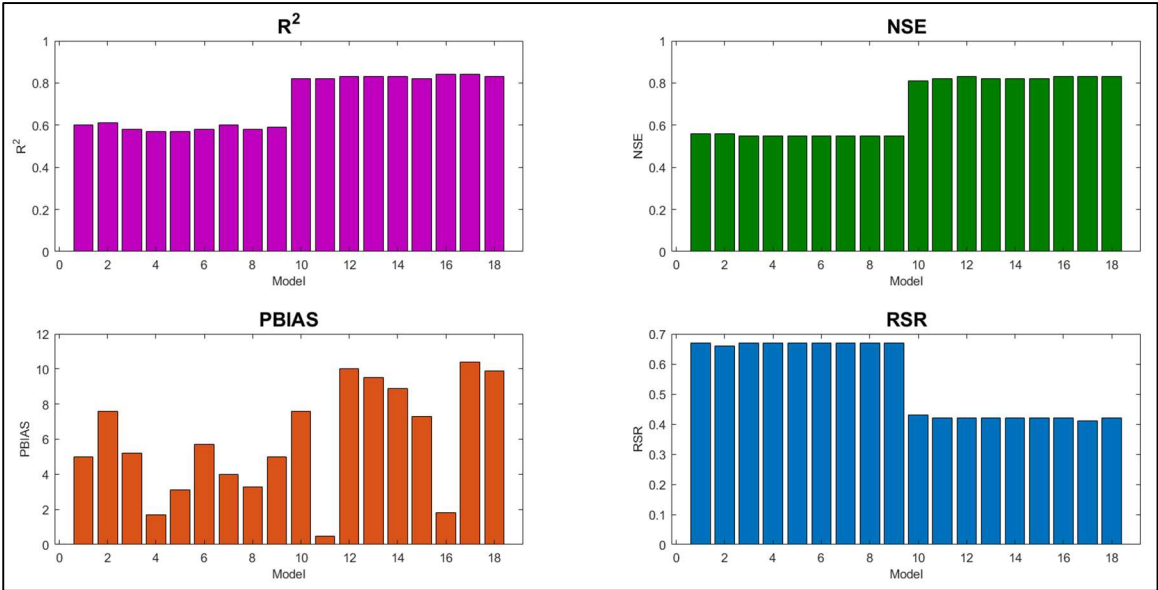


Figure S12: SWAT model performance for the 18 combinations with the four performance criteria (R^2 , NSE, PBIAS, and RSR) for the calibration period

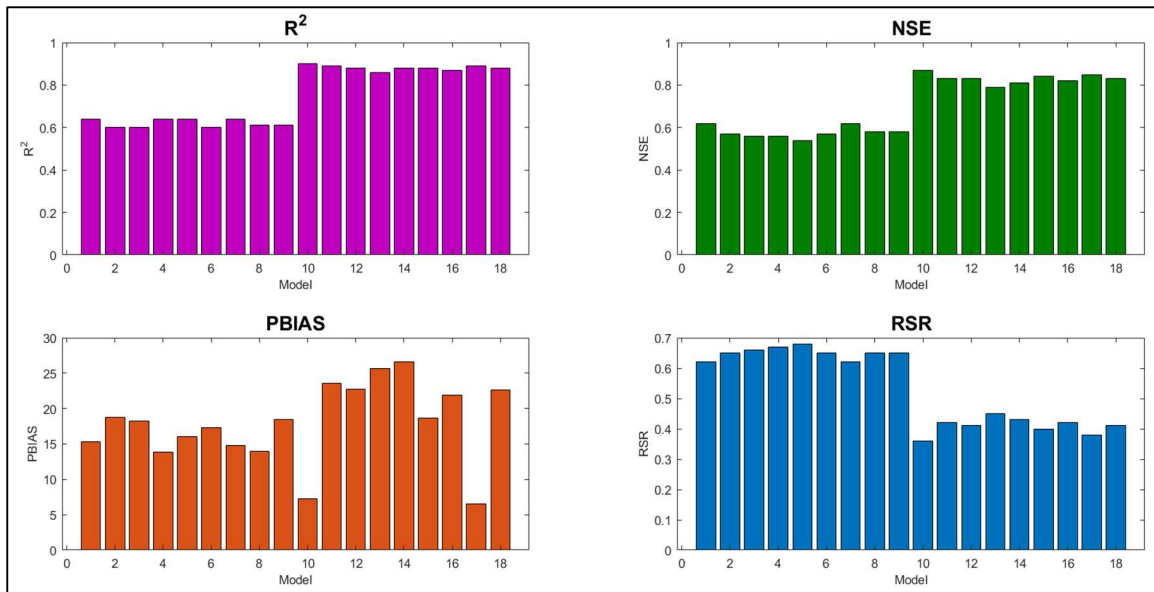


Figure S13: SWAT model performance for the 18 combinations with the four performance criteria (R^2 , NSE, PBIAS, and RSR) for the validation period

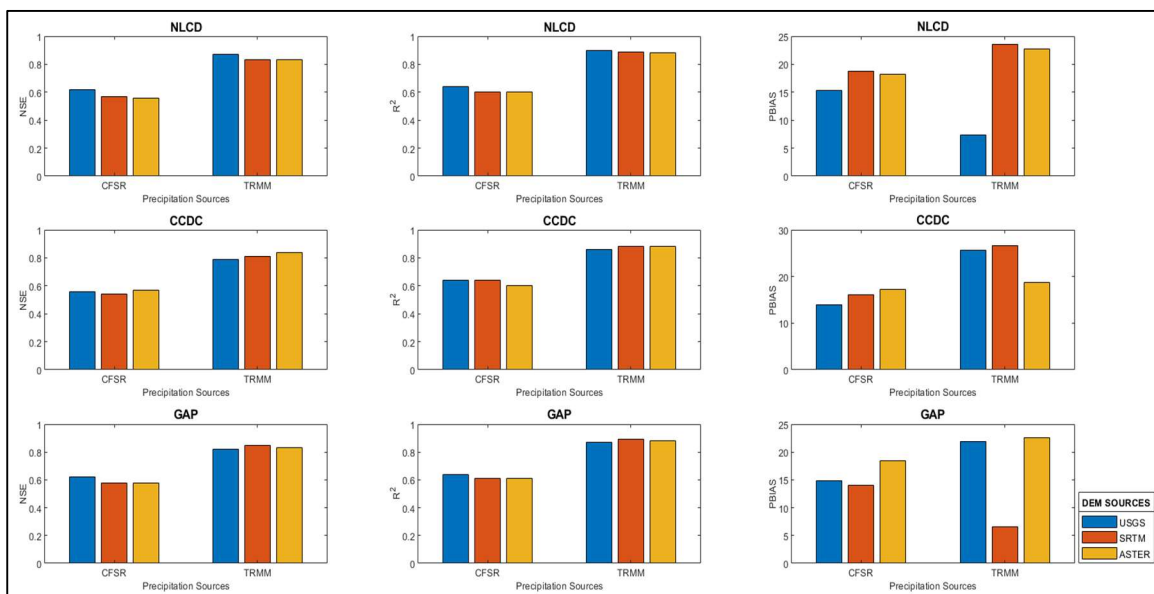


Figure S14: DEM and precipitation dataset comparison based on NSE, R^2 , and PBIAS values for (a) NLCD; (b) CCDC; and (c) GAP LULC

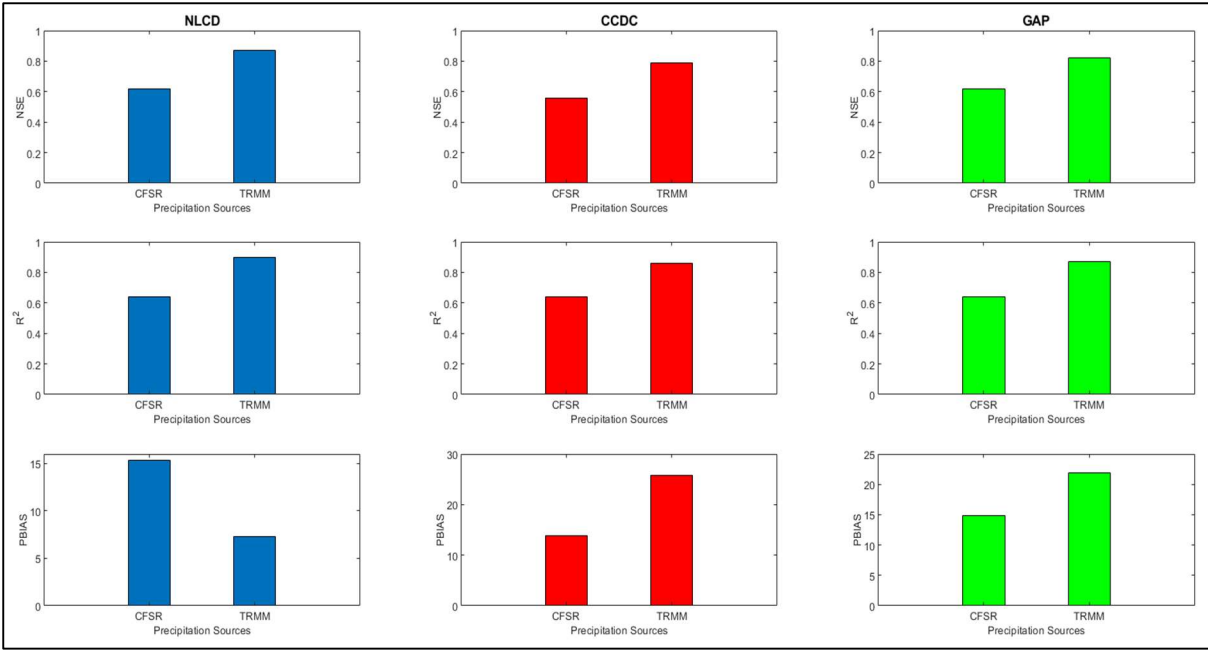


Figure S15: Model performance with various LULC and precipitation dataset combinations for the USGS DEM based on NSE, R^2 , and PBIAS criteria

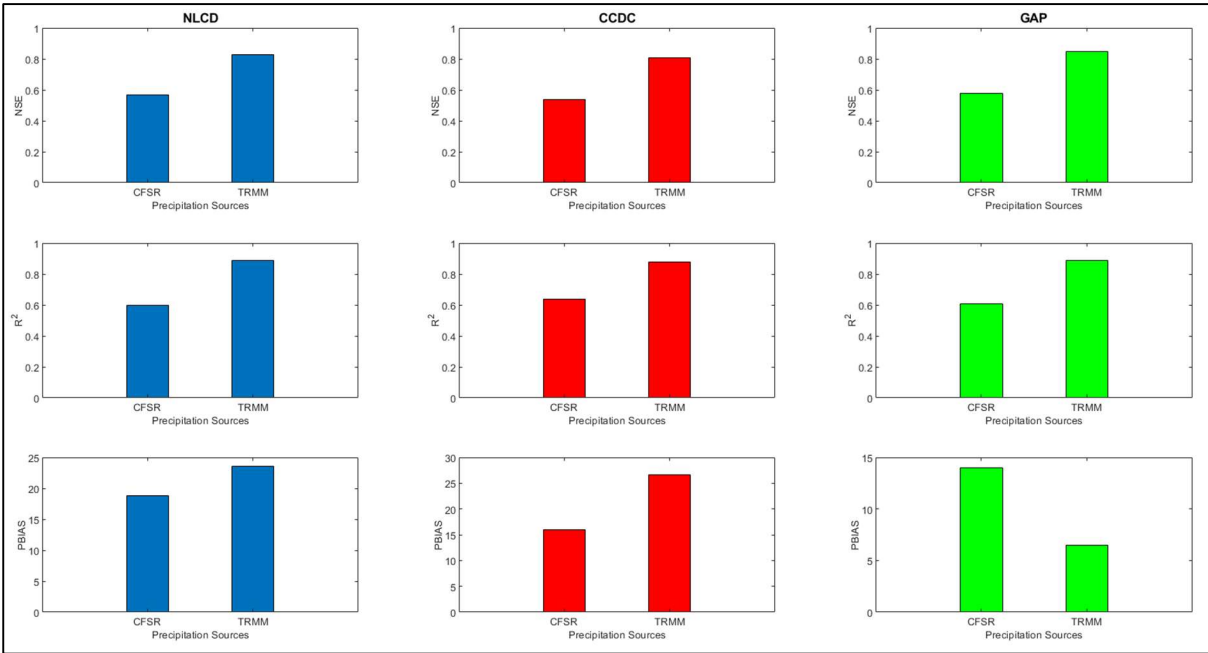


Figure S16: Model performance with various LULC and precipitation dataset combinations for the SRTM DEM based on NSE, R^2 , and PBIAS criteria

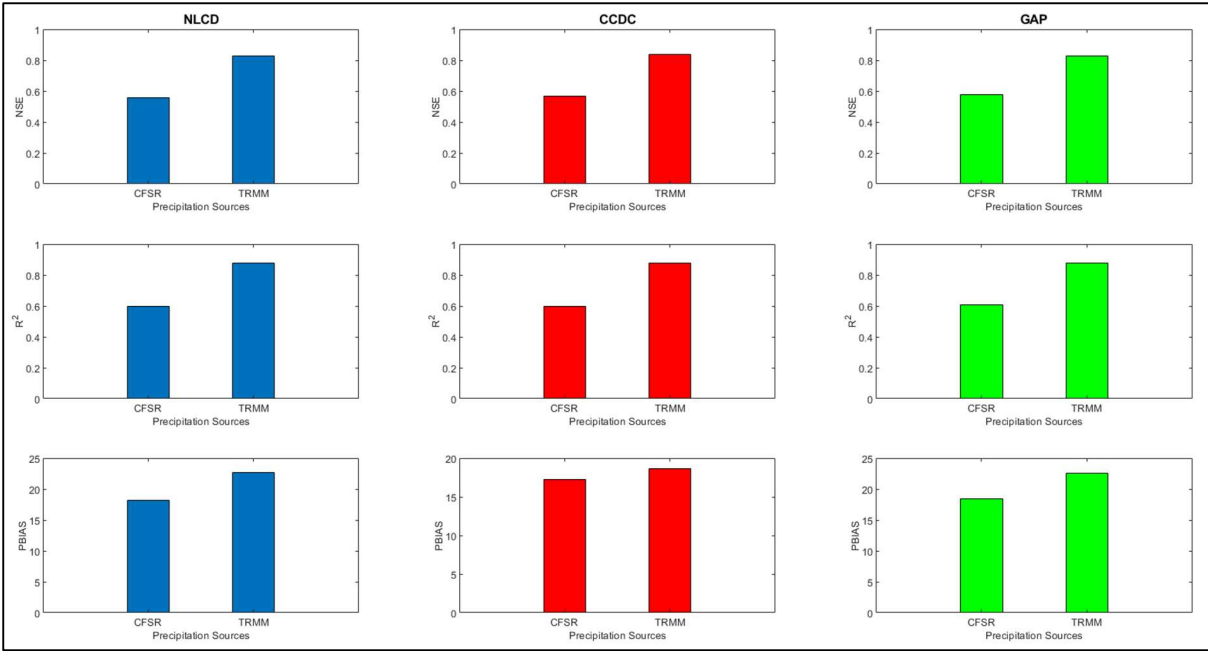


Figure S17: Model performance with various LULC and precipitation dataset combinations for the ASTER DEM based on NSE, R^2 , and PBIAS criteria

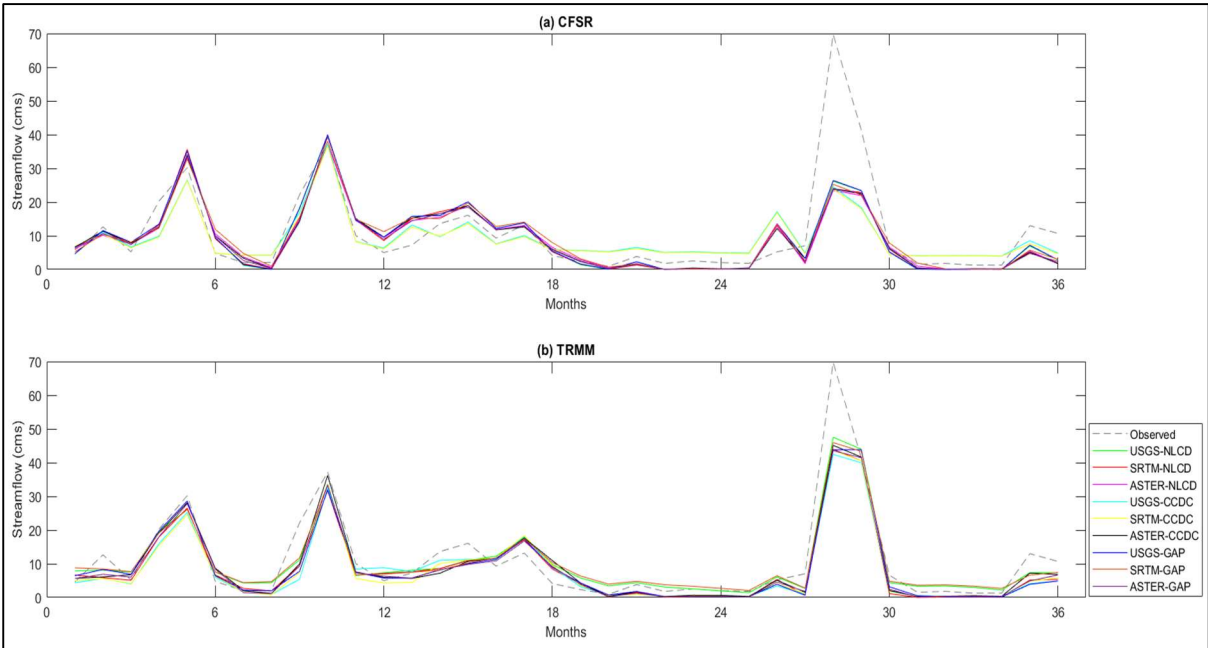


Figure S18: Plots showing the variation of simulated streamflow with the observed streamflow for three different precipitation combinations as (a) CFSR, (b) TRMM

SOUTH FORK WATERSHED RESULTS

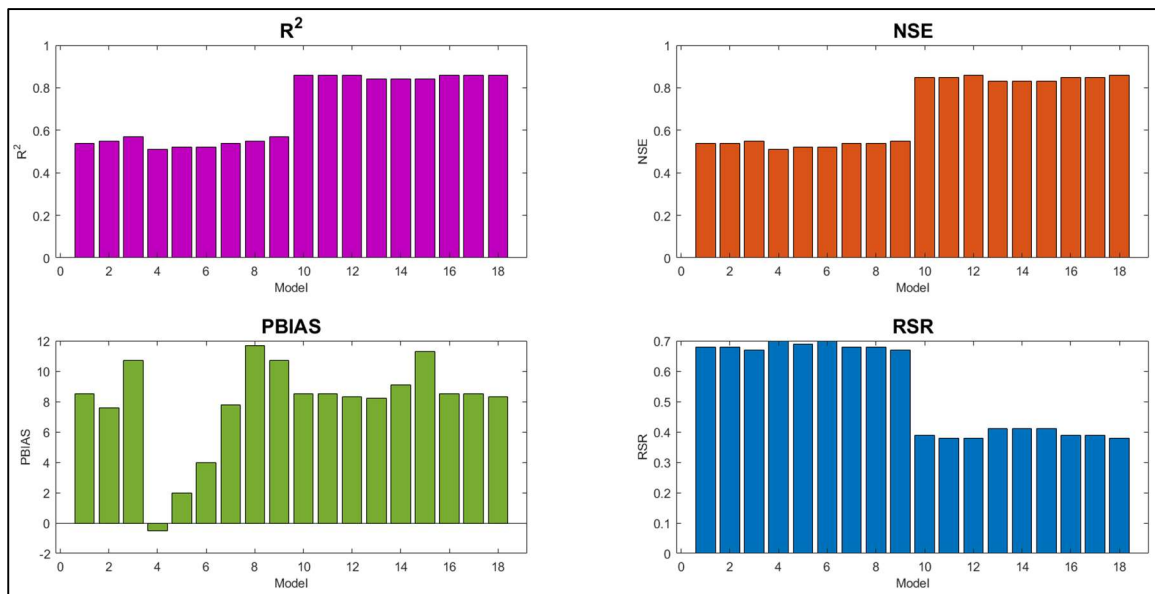


Figure S19: SWAT model performance for the 18 combinations with the four performance criteria (R^2 , NSE, PBIAS, and RSR) for the calibration period

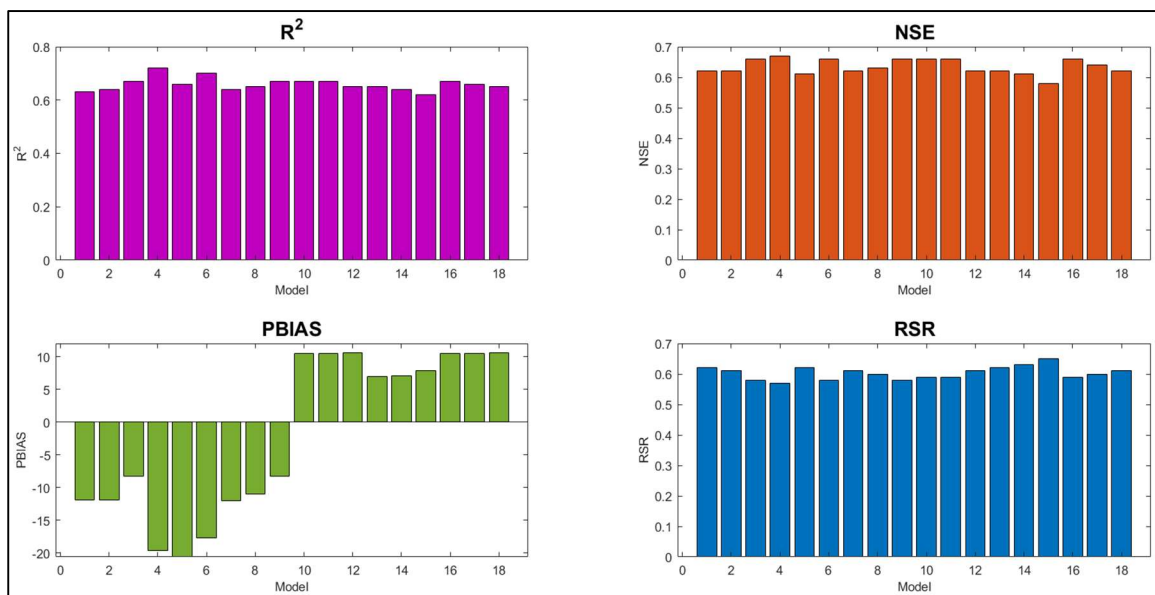


Figure S20: SWAT model performance for the 18 combinations with the four performance criteria (R^2 , NSE, PBIAS, and RSR) for the validation period

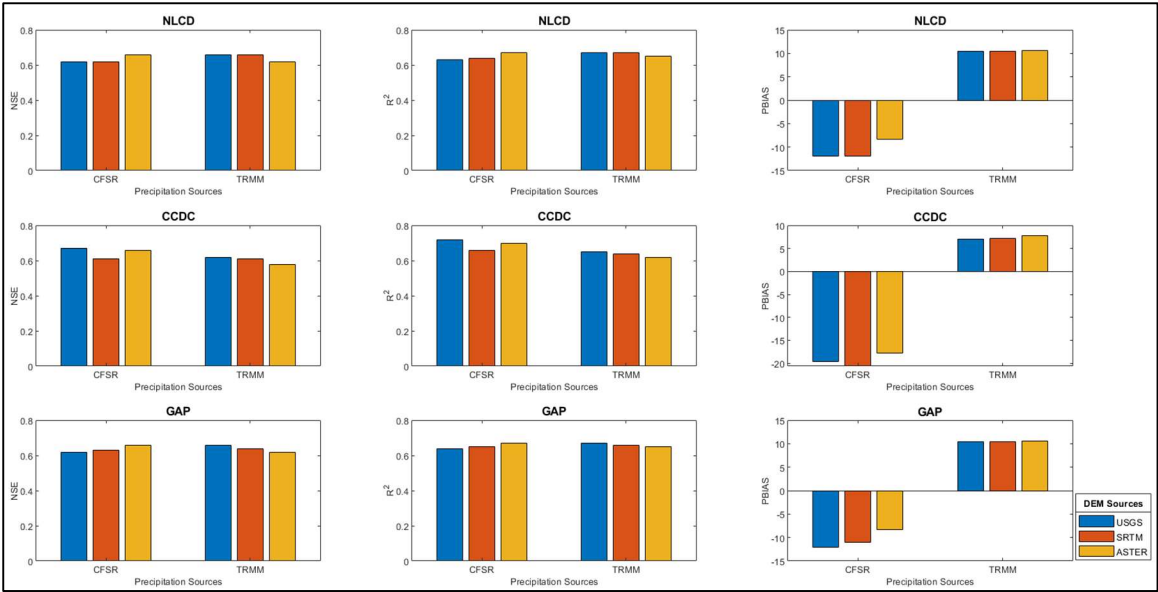


Figure S21: DEM and precipitation dataset comparison based on NSE, R^2 , and PBIAS values for (a) NLCD; (b) CCDC; and (c) GAP LULC

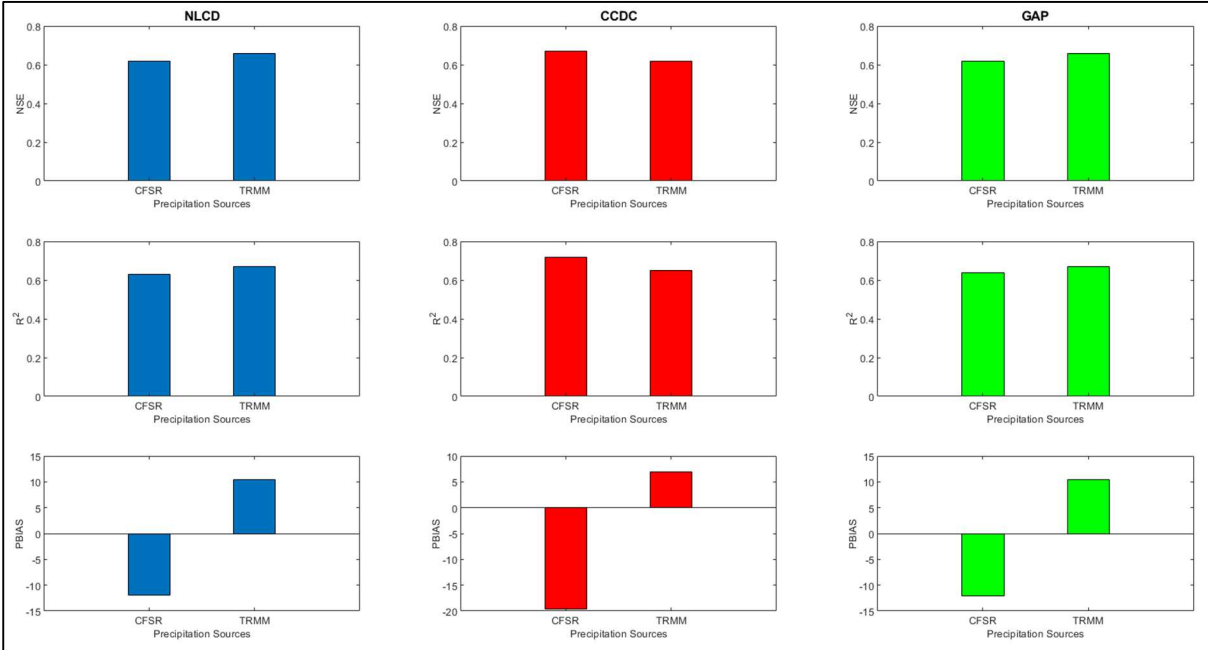


Figure S22: Model performance with various LULC and precipitation dataset combinations for the USGS DEM based on NSE, R^2 , and PBIAS criteria

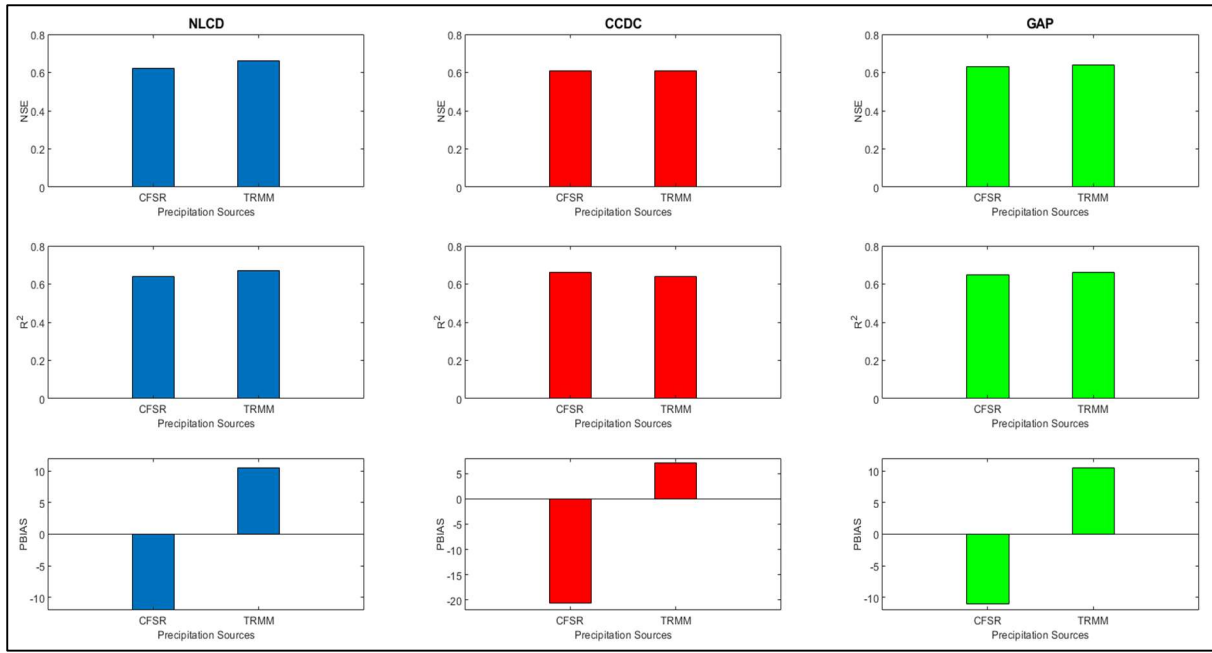


Figure S23: Model performance with various LULC and precipitation dataset combinations for the SRTM DEM based on NSE, R^2 , and PBIAS criteria

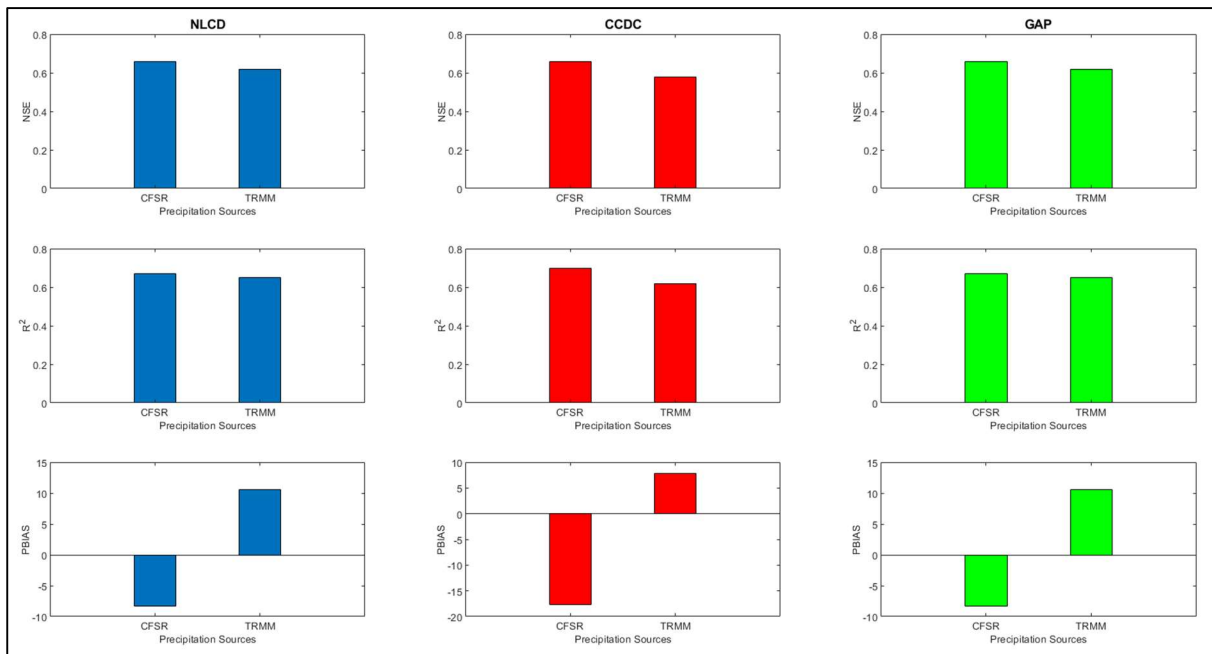


Figure S24: Model performance with various LULC and precipitation dataset combinations for the ASTER DEM based on NSE, R^2 , and PBIAS criteria

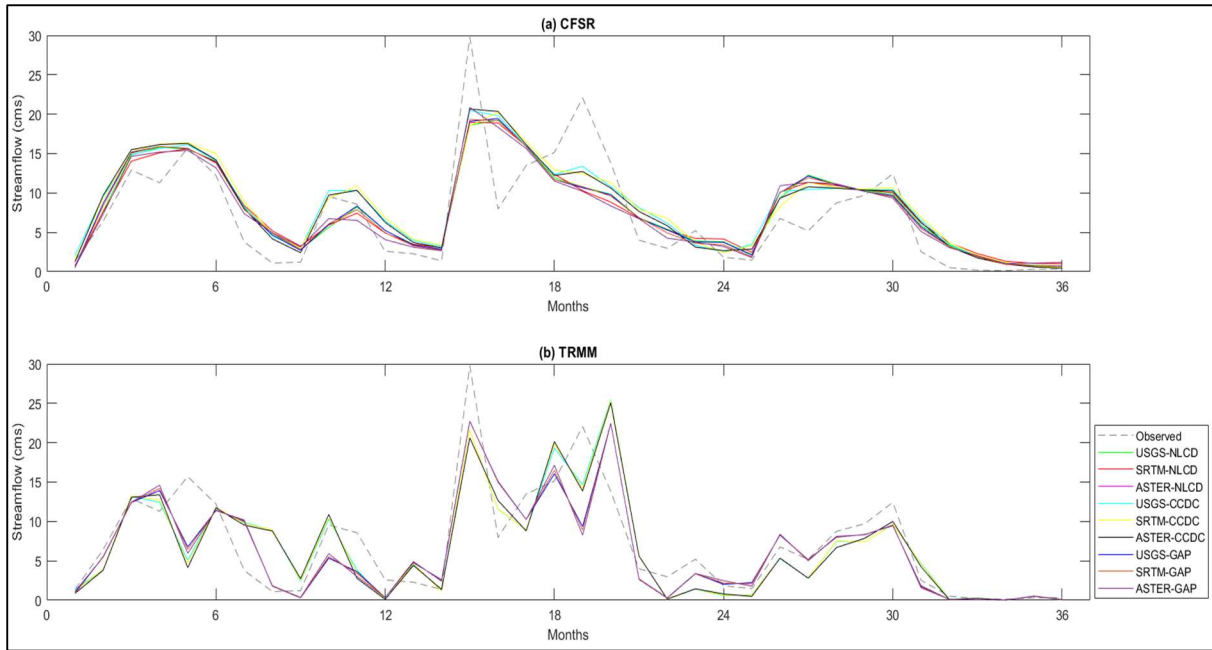


Figure S25: Plots showing the variation of simulated streamflow with the observed streamflow for three different precipitation combinations as (a) CFSR, (b) TRMM

PARAMETER UNCERTAINTY RESULTS

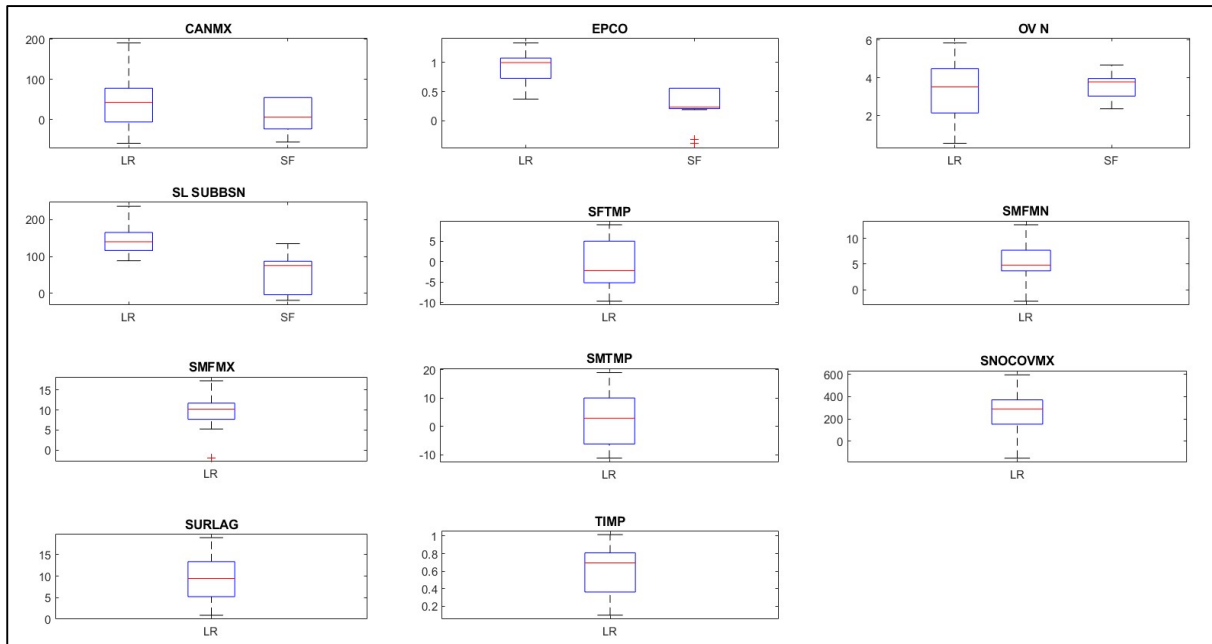


Figure S26: Variation of sensitive parameters for the model combinations used in the two watersheds: (a) Little River (LR) and (b) South Fork (SF), in addition to the nine influential parameters shown in the paper

MCDM RESULTS

Table S1: Input combinations and the corresponding ranking by MCDM analysis for the Peachtree Creek watershed

Combination No.	Combination Name	Ranking by MCDM
9	ASTER_GAP_Gage	1
6	ASTER_CCDC_Gage	2
22	USGS_CCDC_TRMM	3
25	USGS_GAP_TRMM	4
1	USGS_NLCD_Gage	5
19	USGS_NLCD_TRMM	6
3	ASTER_NLCD_Gage	7
20	SRTM_NLCD_TRMM	8
24	ASTER_CCDC_TRMM	9
27	ASTER_GAP_TRMM	9
2	SRTM_NLCD_Gage	10
21	ASTER_NLCD_TRMM	11
23	SRTM_CCDC_TRMM	12
26	SRTM_GAP_TRMM	12
8	SRTM_GAP_Gage	13
5	SRTM_CCDC_Gage	14
4	USGS_CCDC_Gage	15
7	USGS_GAP_Gage	15
15	ASTER_CCDC_CFSR	16
13	USGS_CCDC_CFSR	17
16	USGS_GAP_CFSR	18
14	SRTM_CCDC_CFSR	19
17	SRTM_GAP_CFSR	20
11	SRTM_NLCD_CFSR	21
18	ASTER_GAP_CFSR	22
10	USGS_NLCD_CFSR	23
12	ASTER_NLCD_CFSR	24

Table S2: Input combinations and the corresponding ranking by MCDM analysis for the Little River watershed

Combination No.	Combination Name	Ranking by MCDM
19	USGS_NLCD_TRMM	1
22	USGS_CCDC_TRMM	2
24	ASTER_CCDC_TRMM	3
20	SRTM_NLCD_TRMM	4
21	ASTER_NLCD_TRMM	5

27	ASTER_GAP_TRMM	6
26	SRTM_GAP_TRMM	7
25	USGS_GAP_TRMM	8
2	SRTM_NLCD_Gage	9
6	ASTER_CCDC_Gage	10
23	SRTM_CCDC_TRMM	11
5	SRTM_CCDC_Gage	12
3	ASTER_NLCD_Gage	13
8	SRTM_GAP_Gage	14
4	USGS_CCDC_Gage	15
7	USGS_GAP_Gage	16
1	USGS_NLCD_Gage	17
9	ASTER_GAP_Gage	18
16	USGS_GAP_CFSR	19
11	SRTM_NLCD_CFSR	20
15	ASTER_CCDC_CFSR	21
17	SRTM_GAP_CFSR	22
18	ASTER_GAP_CFSR	23
12	ASTER_NLCD_CFSR	24
10	USGS_NLCD_CFSR	25
13	USGS_CCDC_CFSR	26
14	SRTM_CCDC_CFSR	27

Table S3: Input combinations and the corresponding ranking by MCDM analysis for the Baron Fork watershed

Combination No.	Combination Name	Ranking by MCDM
10	USGS_NLCD_TRMM	1
17	SRTM_GAP_TRMM	2
15	ASTER_CCDC_TRMM	3
16	USGS_GAP_TRMM	4
18	ASTER_GAP_TRMM	5
12	ASTER_NLCD_TRMM	6
11	SRTM_NLCD_TRMM	7
14	SRTM_CCDC_TRMM	8
13	USGS_CCDC_TRMM	9
7	USGS_GAP_CFSR	10
1	USGS_NLCD_CFSR	11
8	SRTM_GAP_CFSR	12
9	ASTER_GAP_CFSR	13
2	SRTM_NLCD_CFSR	14
6	ASTER_CCDC_CFSR	15
3	ASTER_NLCD_CFSR	16

4	USGS_CCDC_CFSR	17
5	SRTM_CCDC_CFSR	18

Table S4: Input combinations and the corresponding ranking by MCDM analysis for the South Fork watershed

Combination No.	Combination Name	Ranking by MCDM
10	USGS_NLCD_TRMM	1
16	USGS_GAP_TRMM	2
11	SRTM_NLCD_TRMM	3
17	SRTM_GAP_TRMM	4
3	ASTER_NLCD_CFSR	5
9	ASTER_GAP_CFSR	6
12	ASTER_NLCD_TRMM	7
18	ASTER_GAP_TRMM	8
13	USGS_CCDC_TRMM	9
14	SRTM_CCDC_TRMM	10
6	ASTER_CCDC_CFSR	11
8	SRTM_GAP_CFSR	12
4	USGS_CCDC_CFSR	13
7	USGS_GAP_CFSR	14
15	ASTER_CCDC_TRMM	15
1	USGS_NLCD_CFSR	16
2	SRTM_NLCD_CFSR	17
5	SRTM_CCDC_CFSR	18